

Application of intense relativistic electron beams to the switching of high currents in high power electrical networks

I. D. Mayergoyz, W. W. Destler, and F. P. Emad
Electrical Engineering Department, University of Maryland, College Park, Maryland 20742

(Received 14 April 1982; accepted for publication 13 July 1982)

A new concept of switching of high currents using intense relativistic electron beams propagating in vacuum drift tubes is presented. Some possible applications of this concept for the design of current switches are discussed. Supporting analytical one-dimensional theory of an electron beam switch is given. Electron beam hysteresis phenomenon associated with the switching mechanism is briefly discussed.

PACS numbers: 41.80.Dd, 52.60.+h, 41.80.-y, 52.80.Vp

I. INTRODUCTION

The principles of construction of reliable high-current switches and fault current limiters have been the focus of considerable research in recent years. This is due to their importance in the protection of expensive power equipment and also in switching power out of inductive storage systems. Among the main advances in this area are the proposed principles based on vacuum arc interruption and on applications of superconductivity to construction of fault current limiters. However, any really difficult problem should be attacked using different approaches. For this reason, other new physical concepts which hold promise for successful switch design are of scientific and practical value.

Below we are proposing a new concept which may be useful for the design of a new kind of electron beam device intended for switching or limiting high currents. In this device, the switching of the current occurs without arc extinguishing and is due to the specific properties of intense relativistic electron beams. This device can be used for switching both dc and ac currents.

The basic element of such a device is a high-power field emission diode. During the past decade, such diodes have been used to investigate applications of intense relativistic electron beams to such diverse areas as microwave and millimeter wave generation,^{1,3} collective ion acceleration,^{4,11} intense ion beam production,¹²⁻¹⁴ and plasma heating.¹⁵ Typically, field emission of electrons occurs when a cold cathode is brought to such a high negative potential relative to ground that the electric field at the surface of the cathode is strong enough to extract electrons from the cathode material. Field emission diodes of this type have been operated at voltages in the range 0.1-15 MeV at current levels of 1-1000 kA, with pulse durations ranging from a few nanoseconds to a few microseconds.

With high power transmission lines already operating in the range 0.1-1 MV at current levels in the kiloampere range, it does not seem unreasonable that field emission diodes could be considered as possible components in novel switching and current interrupting schemes. The work reported in this paper concerns the possible applications of such systems for the switching of high currents in high-power electrical networks. In Sec. II, the basic concept under consideration and its possible applications are presented. Supporting analytical theory is presented in Sec. III.

II. BASIC CONCEPT AND POSSIBLE APPLICATIONS

In the device (see Fig. 1), a high negative voltage is applied to the cathode with respect to the anode. Electrons are field emitted from the cathode, accelerated by the applied voltage, and propagate through the anode hole into a drift region downstream of the anode. Such a relativistic electron beam possesses unique nonlinear properties briefly described below.⁴⁻⁷ If the electron beam current I is below a critical value called the limiting current I_L , the electrons will propagate to the downstream collector, and the full electron beam current will be measured at this point. If $I > I_L$, a region of high electron density called a virtual cathode is formed in close proximity and to the right of the anode. At this point, all current above the threshold value I_L is diverted from the collector to the anode. This phenomenon occurs naturally due to internal properties inherent in intense relativistic electron beams, and does not require any mechanical, solid state, or other switches. Although in theory a current of up to I_L can still propagate to the collector, experimental studies⁵ have shown that in the absence of an applied magnetic field, considerably less than this value is observed at the collector when $I > I_L$. If the distance between anode and

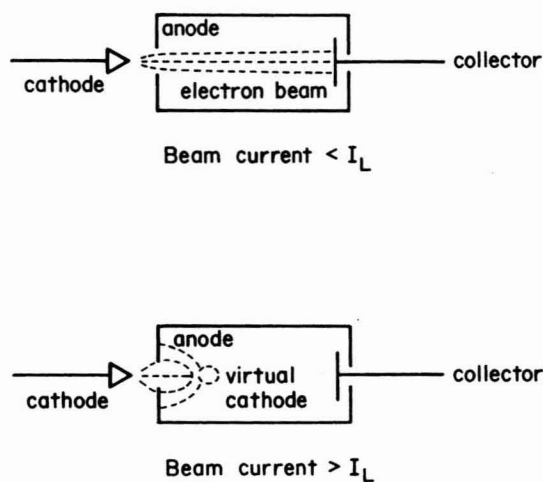


FIG. 1. Schematic of device showing electron trajectories when the beam current is below and above the space-charge-limiting value.

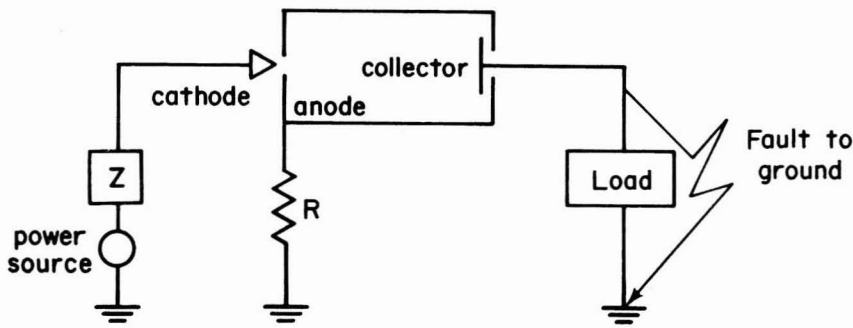


FIG. 2. Schematic of possible application of the device as a current interrupter.

collector is kept relatively small, no magnetic field should be necessary to operate efficiently at $I < I_L$.

The limiting current I_L is a threshold value above which electron current cannot propagate downstream. This current is a function of drift tube geometry and diode voltage and ranges from a few hundred to many thousand amperes. The unique threshold properties of intense relativistic electron beams described above make the use of these electron beams alluring for the switching or limiting of fault currents in power systems, and also for switching power out of inductive storage coils.

One of the possible applications of virtual cathode phenomenon for switching high currents can be viewed as follows (see Fig. 2). During normal service, the electron beam propagates through the drift tube downstream and carries the load current. During a fault, the sudden decrease in load impedance may cause the electron beam current to exceed the limiting current, and a virtual cathode will be formed by means of which most of the fault current is naturally diverted to the anode. If the anode is grounded through a large resistor, then this resistor will absorb the energy and will limit the fault current through the power equipment. Although the described application is the most straightforward, it suffers from the necessity to operate the electron beam device continuously. To overcome this difficulty,

fault-mode operation of this device can be proposed. The advantage of this mode of operation is that the device carries current only during a fault and idles most of the time as it stands guard when needed. A possible circuit for this mode of operation is shown in Fig. 3. Fault-mode operation utilizes the fact that in field-emission diodes, electrons are field emitted from the "cold" cathode only if the applied voltage is above some threshold value. Thus, if the voltage of the auxiliary source (AS) is a little below the threshold value, electron emission will not occur and, consequently, under normal conditions, the current is carried from the power source to the load via CB, a conventional circuit breaker. After a fault, a voltage is induced in the secondary winding of the transformer and the total voltage across the anode-cathode gap exceeds this threshold value. At this time, the electron beam is switched on. The circuit breaker may now be opened without arcing, since the current has an alternate path through the electron beam device. Very soon, the virtual cathode forms and the beam current is diverted to the anode and through resistor R, which absorbs the energy and limits the fault current. It should be emphasized that no switching is required to put the vacuum electron beam device into operation. Small changes in the described scheme are needed to use it for switching power out of inductive storage coils.

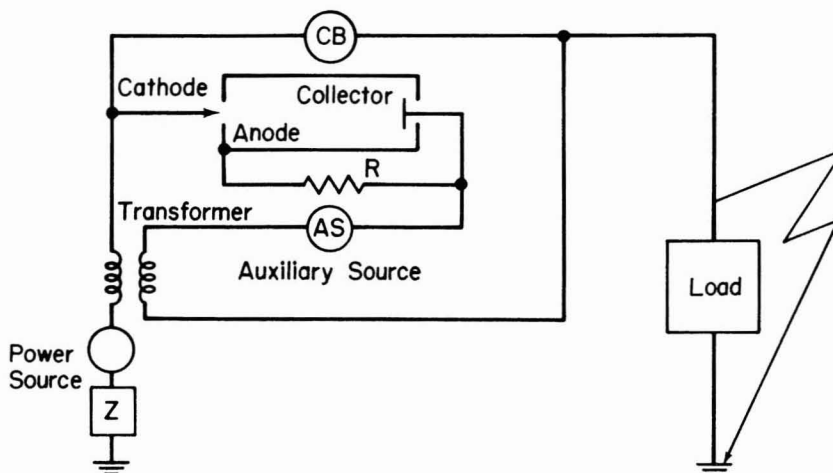


FIG. 3. Schematic of possible application of the device as a current interrupter where the device operates during the fault only.

III. ONE-DIMENSIONAL THEORY FOR THE CALCULATION OF LIMITING AND DIVERTED CURRENTS

A one-dimensional theoretical model of a relativistic nonneutral electron beam propagating between the grounded plane conductors has been treated previously.^{5,6} The operational characteristics of the electron beam device discussed above are different, because the potentials of the collector and anode depend on the transmitted and diverted currents, respectively. As a result, the previous model has been extended to treat these special conditions.

The general configuration which will be discussed is shown in Fig. 4. Two infinite plane conductors are located at $z = 0$ and $z = d$ and are grounded through resistors R_a and R_L , respectively. A relativistic electron beam is injected through the conductor at $z = 0$ with current density $\vec{J}_0 = -J_0\hat{a}_z$. Since a one-dimensional theoretical model is under consideration, the influence of self-magnetic fields is neglected throughout this analysis.

The electrostatic potential $\phi(z)$ between two plane conductors is described by Poisson equation

$$\frac{d^2\phi(z)}{dz^2} = -\frac{\rho(z)}{\epsilon_0}, \quad (1)$$

where ϵ_0 is the permittivity of free space, and the charge density $\rho(z)$ is related to the current density $J(z)$ and velocity $v(z)$ by

$$\rho(z) = \frac{J(z)}{v(z)}. \quad (2)$$

Further it will be convenient to use the relativistic ratio

$$\gamma(z) = \frac{1}{\left(1 - \frac{v^2}{c^2}\right)^{1/2}}. \quad (3)$$

From the energy balance, we find

$$m\gamma c^2 - mc^2 = e[V_a + \phi(z)], \quad (4)$$

where V_a is the anode potential with respect to the cathode. From (1) through (4) and using the current continuity equa-

tion, we obtain

$$\frac{d^2\gamma}{dz^2} = \frac{eJ_0}{mc^3\epsilon_0} \frac{\gamma}{(\gamma^2 - 1)^{1/2}}, \quad (5)$$

where J_0 is the density of the injected current. Now, let us subdivide the volume between the conducting planes into two parts: (1) domain $z < d_m$ before the position of the potential minimum and (2) domain $z > d_m$ after the position of the potential minimum. Integrating (5) over each of these domains and taking into account that $[d\gamma/dz]_{z=d_m} = [d\phi/dz]_{z=d_m} = 0$, we derive

$$\frac{d\gamma}{dz} = -\left(\frac{2eJ_0}{\epsilon_0 mc^3}\right)^{1/2} [(\gamma^2 - 1)^{1/2} - (\gamma_m^2 - 1)^{1/2}]^{1/2} \quad z < d_m, \quad (6)$$

$$\frac{d\gamma}{dz} = \left(\frac{2eJ_0}{\epsilon_0 mc^3}\right)^{1/2} [(\gamma^2 - 1)^{1/2} - (\gamma_m^2 - 1)^{1/2}]^{1/2} \quad z > d_m, \quad (7)$$

where γ_m corresponds to the potential minimum ϕ_m and according to (3) and (4), it is given by

$$\gamma_m = 1 + \frac{e(V_0 + \phi_m)}{mc^2}. \quad (8)$$

In (8), the fact that $V_a = V_0$ has been taken into account, because there is no diverted current. By integrating (6) and (7), we obtain

$$\int_{\gamma_m}^{\gamma_0} \frac{d\gamma}{[(\gamma^2 - 1)^{1/2} - (\gamma_m^2 - 1)^{1/2}]^{1/2}} = \left(\frac{2eJ_0}{\epsilon_0 mc^3}\right)^{1/2} d_m, \quad (9)$$

$$\int_{\gamma_m}^{\gamma_c} \frac{d\gamma}{[(\gamma^2 - 1)^{1/2} - (\gamma_m^2 - 1)^{1/2}]^{1/2}} = \left(\frac{2eJ_0}{\epsilon_0 mc^3}\right)^{1/2} (d - d_m), \quad (10)$$

where

$$\gamma_0 = 1 + \frac{eV_0}{mc^2}, \quad (11)$$

$$\gamma_c = 1 + \frac{e(V_0 + \phi_c)}{mc^2}. \quad (12)$$

In (12), ϕ_c is the potential of the collector. For this potential, we have

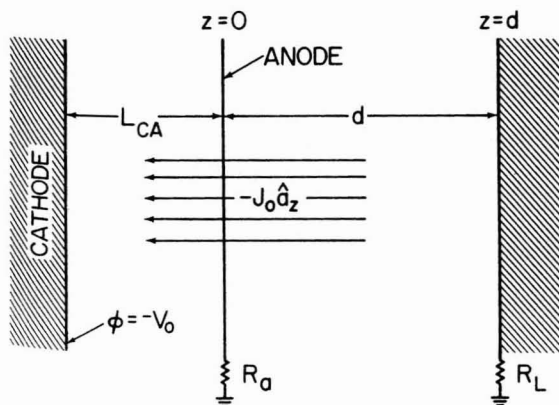


FIG. 4. Configuration used for one-dimensional theoretical analysis.

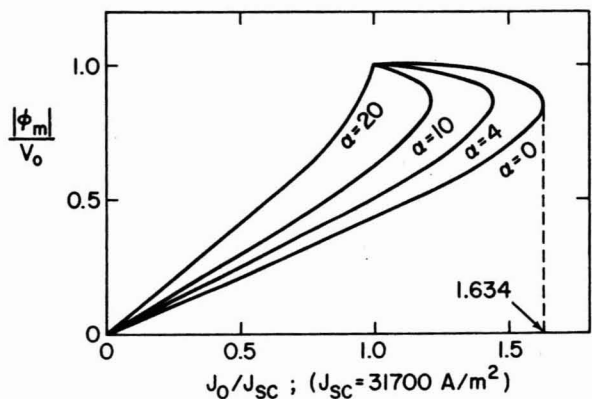


FIG. 5. Theoretical plots of minimum potential (relative to V_0) vs injected current density (relative to the space charge limiting value) for several values of the parameter α .

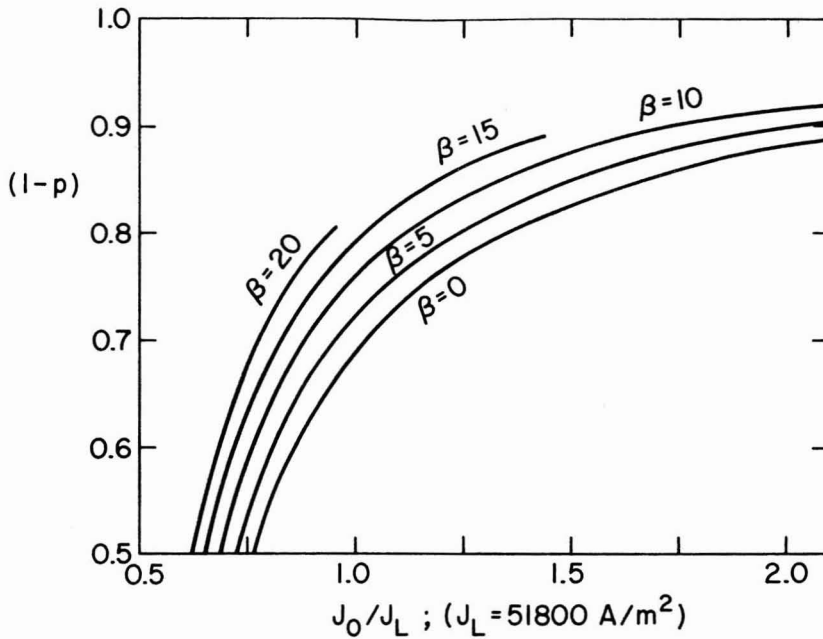


FIG. 6. Fraction of current diverted to the anode vs the injected current (relative to the limiting value) for several values of the parameter β .

we have

$$\phi_c = -J_0 S R_L = -J_0 \alpha, \quad (13)$$

where S is the area of the beam cross section. From (12) and (13), it follows that

$$\gamma_c = 1 + \frac{e(V_0 - J_0 \alpha)}{mc^2}. \quad (14)$$

Substituting (14) into (10) and excluding d_m from Eqs. (9) and (10), we obtain

$$\int_{\gamma_m}^{1 + e(V_0 - J_0 \alpha)/mc^2} \frac{d\gamma}{[(\gamma^2 - 1)^{1/2} - (\gamma_m^2 - 1)^{1/2}]^{1/2}} = \left(\frac{2eJ_0}{\epsilon_0 mc^3}\right)^{1/2} d - \int_{\gamma_m}^{\gamma_0} \frac{d\gamma}{[(\gamma^2 - 1)^{1/2} - (\gamma_m^2 - 1)^{1/2}]^{1/2}}. \quad (15)$$

This is the nonlinear equation which relates γ_m (or the corresponding potential minimum ϕ_m) to the density J_0 of the injected current. Assuming different values of $|\phi_m|/V_0$, we can solve this nonlinear Eq. (15) and find the corresponding value of J_0 . The value of J_0 which corresponds to $\phi_m = -V_0$ is called the space-charge-limited current density J_{sc} , because it is equal to the value obtained from the relativistic Child Law obtained by Jory and Trivelpiece¹⁶ for space-charge-limited flow in a diode with an effective anode-cathode distance equal to $d/2$. Equation (15) has been used for the calculations. Characteristic curves obtained from this equation are presented in Fig. 5, where the absolute value of normalized minimum potential $|\phi_m|/V_0$ is plotted vs J_0/J_{sc} for several values of α measured in ohm m^2 . The calculations have been performed for $V_0 = 1$ MV and $d = 0.5$ m. The allowable maximum values of J_0 correspond to the values of limiting current I_L . The curves also provide information

concerning the dependence of the limiting current I_L on the load R_L . According to these curves, it follows that the limiting current is always greater than or equal to the space-charge-limited current. In this context, it is evident that normal ($I < I_L$) operation of this device is possible if the current through the device is below its space-charge-limited value.

Now, let us consider the case of fault operation when the injected current is above its limiting value. Then, the virtual cathode with $\phi_m = -V_0$ is formed at $z = d_m$. This virtual cathode diverts the main part of the injected current to the anode. The diverted current flows through the resistor R_a and results in a decrease in the anode potential value.

In order to determine the time-averaged properties of the system, we assume that $1 - p$ is the fraction of injected current that is reflected.

Then the charge density can be expressed as

$$\rho(z) = \begin{cases} (p - 2)J_0/v(z) & z < d_m \\ -pJ_0/v(z) & z > d_m. \end{cases} \quad (16)$$

From (16) and (1) through (4), we derive

$$\frac{d^2\gamma}{dz^2} = \frac{e(2-p)J_0}{\epsilon_0 mc^3} \frac{\gamma}{(\gamma^2 - 1)^{1/2}}, \quad z < d_m, \quad (17)$$

$$\frac{d^2\gamma}{dz^2} = \frac{epJ_0}{\epsilon_0 mc^3} \frac{\gamma}{(\gamma^2 - 1)^{1/2}}, \quad z > d_m. \quad (18)$$

As previously, integrating (17) and (18) and taking into account that in this case $\gamma_m = 1$, we find

$$\int_1^{\gamma_a} \frac{d\gamma}{(\gamma^2 - 1)^{1/4}} = \left(\frac{2e(2-p)J_0}{\epsilon_0 mc^3}\right)^{1/2} d_m, \quad (19)$$

$$\int_1^{\gamma_0} \frac{d\gamma}{(\gamma^2 - 1)^{1/4}} = \left(\frac{2epJ_0}{\epsilon_0 mc^3}\right)^{1/2} (d - d_m), \quad (20)$$

here

$$\gamma_a = 1 + \frac{e[V_0 - (1-p)\beta J_0]}{mc^2}, \quad (\beta = SR_a) \quad (21)$$

and $\gamma_c = \gamma_0$, because in the case of fault operation the resistor R_L is shunted and the collector potential with respect to cathode is equal to V_0 .

Substituting (21) into (19) and excluding d_m from (19) and (20), we derive

$$\left(\frac{2epJ_0}{\epsilon_0 mc^3}\right)^{1/2} d - \left(\frac{p}{2-p}\right)^{1/2} \int_1^{1+e[V_0-(1-p)\beta J_0]/mc^2} \frac{d\gamma}{(\gamma^2-1)^{1/4}} = \int_1^{\gamma_0} \frac{d\gamma}{(\gamma^2-1)^{1/4}} \quad (22)$$

For given V_0 , J_0 , and β , Eq. (22) can be regarded as a nonlinear equation which can be solved for the fraction p of the beam current transmitted. Using this equation, the fraction $1-p$ of the current diverted has been calculated for $V_0 = 1$ MV and different values of β and J_0 . The results of calculations are presented as curves shown in Fig. 6. The curves corresponding to $\beta = 20 \text{ ohm m}^2$ and $\beta = 15 \text{ ohm m}^2$ are presented only for those values of J_0 for which the anode potential remains positive.

From these results, it follows that reflected current exists even for values of the injected current less than the limiting current. The calculations show that the reflected current is equal to zero when the injected current approaches its space-charge-limited value. At first, this result seems to be contradictory to the calculations presented in Fig. 5. But, in fact, there is no contradiction and these results can be physically explained as follows. The curves given in Fig. 5 correspond to the situation when the injected current is continuously increasing from zero to its limiting value I_L . The curves given in Fig. 6 have been calculated under the assumption that the virtual cathode is formed. Consequently, these curves can be interpreted as corresponding to the continuous decrease in the injected current from a value above the limiting current to the value of the space-charge-limited current. Thus, different values of the reflected (or transmitted) current correspond to one and the same value of the injected current for the cases of continuously increasing and continuously decreasing injected current. This phenomenon can be construed as electron beam hysteresis, as shown schematically in Fig. 7. The physical mechanism of the irreversibility mentioned above consists of the fact that different charge distributions (different states) correspond to one and the same limiting current when this current is approached from below or above, respectively. Thus, in order to form the virtual cathode, an injected current above the limiting current is required. To maintain the virtual cathode, however, injection currents only above the space-charge-limited value are needed. It is interesting to note that the hysteresis loop shown in Fig. 7 is unusual in that bistability occurs only on the ascending branch. This phenomena has been investigated nonrelativistically¹⁷ previously. Another relativistic discussion of electron beam hysteresis has been reported by Sullivan *et al.*¹⁸

IV. CONCLUSIONS

The concept of using a virtual cathode formed by an intense electron beam propagating in vacuum as a switch for high-power electric network applications appears to be

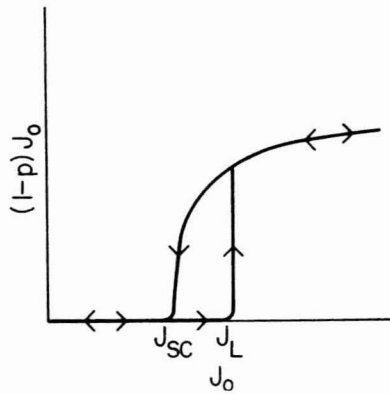


FIG. 7. Schematic of electron beam hysteresis phenomenon.

sound theoretically within the limits of the one-dimensional theory presented. One-dimensional numerical simulations of virtual cathode behavior in such systems show the formation of a virtual cathode which oscillates both in axial position and in amplitude about average values predicted by analytical theory.⁵ Two-dimensional effects will doubtless affect the magnitudes of the transmitted and diverted currents predicted by the one-dimensional analysis, but the basic operational characteristics should remain qualitatively the same. The operating parameters of such a device appear well within the range of those found in high-power transmission line systems in commercial use, and very high percentages of an initial current value may be diverted to a dump resistor in this manner. The practical limits of such a device (required vacuum, pulse length, etc.) are primary targets for future experimental investigation.

ACKNOWLEDGMENTS

The authors are grateful for useful discussions with Professor M. Reiser, Professor C. D. Striffler, Dr. John Grossman, R. Kulkarni, and A. Bromborsky. This work was supported in part by The Air Force Office of Scientific Research, The U.S. Department of Energy, and the University of Maryland Computer Center.

- ¹G. Bekefi and T. Orzechowck, *Phys. Rev. Lett.* **37**, 379 (1976).
- ²V. L. Granatstein, P. Sprangle, M. Herndon, R. K. Parker, and S. P. Schlesinger, *J. Appl. Phys.* **46**, 3800 (1975).
- ³W. W. Destler, R. C. Weiler, and C. D. Striffler, *Appl. Phys. Lett.* **38**, 570 (1981).
- ⁴J. W. Poukey and N. Rostoker, *Plasma Phys.* **13**, 897 (1971).
- ⁵W. W. Destler, H. S. Uhm, H. Kim, and M. P. Reiser, *J. Appl. Phys.* **50**, 5 (1979).
- ⁶V. S. Voronin, Yu. T. Zozulya, and A. N. Lebedev, *Sov. Phys. Tech. Phys.* **17**, 432 (1972).
- ⁷C. L. Olson, *Phys. Fluids* **18**, 585 (1975).
- ⁸J. S. Luce, *Ann. N. Y. Acad. Sci.* **251**, 217 (1975).
- ⁹S. E. Graybill and J. R. Uglum, *J. Appl. Phys.* **41**, 236 (1970).
- ¹⁰J. M. Grossmann, I. D. Mayergoz, and C. D. Striffler, *IEEE Trans. Nucl. Sci.* **28**, 3 (1981).
- ¹¹W. W. Destler, L. E. Floyd, and M. Reiser, *Phys. Rev. Lett.* **44**, 70 (1980).
- ¹²J. M. Neri, D. A. Hammer, and J. B. Greenly, *Bull. Am. Phys. Soc.* **26**, 899 (1981).
- ¹³C. W. Mendel, J. P. Quintenz, and J. W. Poukey, *Bull. Am. Phys. Soc.* **26**, 900 (1981).

- ¹⁴F. L. Sandel, S. J. Stephanakis, D. Mosher, and P. F. Ottinger, *Bull. Am. Phys. Soc.* **26**, 1010 (1981).
- ¹⁵C. A. Kapetanakis and W. M. Black, *Bull. Am. Phys. Soc.* **18**, 1264 (1973).
- ¹⁶H. R. Jory and A. W. Trivelpiece, *J. Appl. Phys.* **40**, 3924 (1969).
- ¹⁷See, for example, *Electron Dynamics of Diode Regions*, edited by C. U.

Birdsall and W. B. Bridges (Academic, New York, 1966).

¹⁸D. J. Sullivan and E. A. Coutsias, *Proceedings of the 4th International Topographical Conference on High-Power Electron and Ion Beam Research and Technology*, June 29–July 3, 1981 (Palaiseau, France), Vol. I, p. 371.